International Journal of Science and Research (IJSR)
ISSN (Online): 2319-7064
Index Copernicus Value (2013): 6.14 | Impact Factor (2015): 6.391

Single Crystal EPR and Optical Studies of VO (II) Ion Doped in Triglycine Acetate

M. S. Balamurugan[1], S. Boobalan[2], P. Subramanian[3]

[1]Department of Physics, JCT College of Eng. & Tech., Coimbatore – 638 105, India

[2]Department of Chemistry, J.J. College of Eng. & Tech. Tiruchirappalli – 620 009, India

[3]Department of Physics, Gandhigram Rural University, Gandhigram – 624 302, India

Abstract: ***Electron paramagnetic resonance studies on single crystals of Triglycine acetate doped with VO(II) are carried out in the room temperature at X-band frequencies. Single crystal rotation in each of the three mutually orthogonal crystallographic planes namely ab, ac* and bc* indicate two chemically equivalent sites, with differing intensities. Angular variation studies in all the three orthogonal planes confirm that the two intense vanadyl sites referred as I and II, are found to be magnetically inequivalent, have occupied interstitial positions in the lattice. The spin Hamiltonian parameters obtained for the two sites are Site I: g_{xx}=1.9818; g_{yy}=1.9646; g_{zz}=1.9346; A_{xx}=7.295 mT; A_{yy}=6.396 mT; A_{zz}= 18.456 mT. Site II: g_{xx}=1.9815; g_{yy}=1.9713; g_{zz}=1.9348; A_{xx}=5.609 mT; A_{yy}= 7.140 mT; A_{zz} =17.942 mT. However the analysis of the powder spectrum reveals the presence of only one site. Admixture coefficients, Fermi contact and dipolar interaction terms have also been evaluated. UV-Visible data of doped complex confirm the structure and symmetry of the host lattice.***

Keywords: crystal growth; single crystal EPR studies; optical studies;

1. Introduction

Non-Linear Optical (NLO) material for optical second harmonic generation (SHG) have received consistent attention for applications in the field of telecommunication, optical computing, optical information processing, optical disk data storage, laser remote sensing, laser driven fusion, color displays material diagnostics and optical switches in inertial confinement laser fusion experiments [1-6]. In general, organic materials (amino group) show a good efficiency for SHG. Most organic NLO crystals have usually poor mechanical and thermal properties and are susceptible to damage in applications. It is difficult to grow large optical quality crystals of these materials for device applications. Crystals of amino acids are good candidates for NLO application. In recent years Electron Paramagnetic Resonance (EPR) has been used as a tool to identify paramagnetic transition metal ions, trapped hole centers and electrons close to the conduction states in non-linear optical and photorefractive materials [7-9].

Vanadyl ion is the most stable biatomic ion [10] among a few molecular paramagnetic transition metal ions which is used extensively as an impurity probe for electron paramagnetic resonance studies. Due to short V=O bond, the unpaired electron is in a nondegenerate state. This leads to resolved electron paramagnetic resonance (EPR) spectra. The hyperfine interaction is anisotropic and therefore sensitive to orientation, conformation, and rotational relaxation [11]. As a result, interesting changes are found in the EPR and optical spectrum in different crystalline field environments [12–16].

Since, to our knowledge, there is no EPR data seem to exist for VO(II) ions introduced in diamagnetic glycine-organic acid compounds and in this work we report an EPR and optical study of VO(II) dopant ions in the single crystals of Triglycine acetate (hereafter abbreviated as TGA) [17] whose crystal structure details are used for EPR.

2. Experimental

2.1 Crystal Growth

Single crystals of TGA were prepared by using the following procedure. The starting materials glycine and glacial acetic acid were taken in the ratio 3:1. The calculated amount of salt was dissolved in deionized water at room temperature with continuous stirring [17]. One percent by weight of vonadyl sulphate was added as dopant during crystal growth. The synthesized solution was left to dry at room temperature. Single crystals of VO(II)/TGA were obtained within 15 days by slow evaporation of the solution at room temperature.

2.2 Crystal Structure

TGA belongs to monoclinic crystal symmetry, and having unit cell parameters a = 0.5102 nm, b = 1.1970 nm, c = 0.5461 nm, $\alpha = \gamma = 90°$, $\beta = 111.7665°$. The cell volume V = 309.7863 Å^3.

2.3 EPR Recording

EPR spectra were recorded at room temperature using a JEOL JES TE100 ESR spectrometer operating at X-band frequency, having a 100 kHz field modulation. Single crystal of VO(II) doped TGA with proper shape and size was selected for rotations in the three mutually orthogonal planes namely *ab*, *ac** and *bc**. Angular variations of the crystal were made at room temperature by rotating the single crystal along the three mutually orthogonal axes *a*, *b* and *c**.

2.4 Optical adsorption Spectroscopy:

Powder sample of VO(II)/TGA was used for optical absorption studies and the spectrum was recorded at room temperature using a Varian Cary 5000 UV-Visible NIR spectrometer in the range of 200–1100 nm.

3. Results and Discussion

Single crystal EPR studies were carried out at room temperature for VO(II) ion doped TGA with proper shape and size. Rotations are carried out in the three mutually orthogonal planes namely *ab*, *ac** and *bc** to obtain spin Hamiltonian parameters. Here, *b* corresponds to crystallographic axis *b*, *a* is perpendicular to axis *b* in *ab* plane whereas *c** is perpendicular to both the axes *a* and *b*. Fig. 1a shows a typical EPR spectrum of VO(II)/TGA, at a particular orientation in plane I (*bc**of site I at θ = 70˚ and *ac** of site II at θ = 120˚). The EPR spectrum consists of eight major lines characteristic of a VO(II) ion with S = 1/2 and I = 7/2. During crystal rotations, the observation of splitting of hyperfine lines indicates the presence of another site. Crystal rotations were done in all the three planes (say Plane 1) to obtain spin Hamiltonian parameters. Another EPR spectrum of the complex, at the indicated orientation, is shown in Fig. 1b for the plane II (*ac**of site I at θ = 30˚ and *ab* of site II at θ = 50˚). Here, one can notice the two sites (Sites I and II). Fig. 1c represents the Single crystal EPR spectrum of VO(II)/TGA at room temperature for plane III (*ab* of site-I at θ = 110˚ and *bc** of site-II at θ = 10˚). Generally, the coincidence of two sites along crystallographic axes suggests that the two sites are magnetically inequivalent but chemically equivalent. In order to confirm this observation, isofrequency plots were plotted in the three planes and are given in Fig. 2a, 2b and 2c respectively. In all these figures, closed circles (–●-●-) indicates Site-I and open circles (–o-o-o-) indicates Site-II. A close look at Fig. 1b suggests that one site has considerable g anisotropy, whereas the other site has relatively lower g anisotropy. The difference is also noticed in hyperfine values. Normally, during crystal rotations, when the system has two sites, which are magnetically inequivalent, but chemically equivalent, but the anisotropy in g and A should be the same. Hence, the rotation of crystals have been labeled as Plane I, II and III, instead of normal way (*ab*, *ac** and *bc**).

The spectra obtained in the three orthogonal planes for VO(II) ion are fitted with the following spin-Hamiltonian using the program EPR – NMR [18]

$$\hat{H} = \beta(g_x B_x S_x + g_y B_y S_y + g_z B_z S_z) + A_x S_x I_x + A_y S_y I_y + A_z S_z I_z$$

The *g* and *A* matrices thus calculated are given in Table 1, along with the principal values and direction cosines. Using these *g* and *A* matrices, the isofrequency plots are simulated for three planes namely *ac**, *bc** and *ab* and are given in Fig. 2a, 2b and 2c respectively, where a good agreement is noticed. In all these figures, the solid lines indicate the theoretical values and the solid and open circles indicate the experimental values of site-I and site-II respectively.

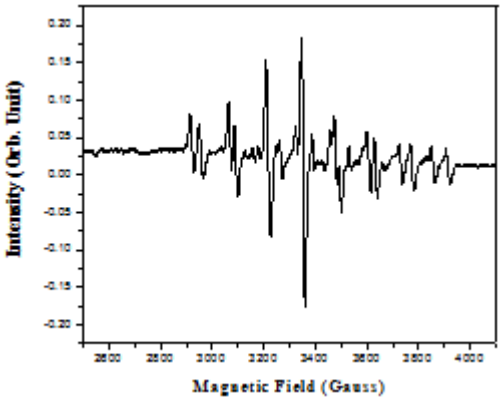

Figure 1 (a): Single crystal EPR spectrum of VO(II)/ TGA at room temperature for plane I (*bc**of site I at θ = 70˚ and *ac** of site II at θ = 120˚) , ν = 9.4060 GHz.

The direction cosine of C – O, C – C and C – N bonds in TGA lattice are given in Table 2. These are helpful to predict the location of the paramagnetic impurity. If the direction cosines of principal value of g_{zz} match with any one of the direction cosines of bonds in TGA, one can assume that the dopant has entered the lattice substitutionally. Otherwise, an interstitial location is expected for the paramagnetic impurity. A close look at the direction cosines given in Tables 1 and 2 indicate that none of them matches with each other. In other words, one can suggest that the vanadyl ion might have entered the lattice in an interstitial location.

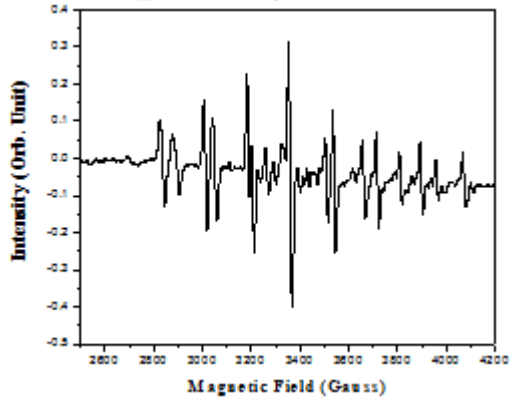

Figure 1(b): Single crystal EPR spectrum of VO(II)/TGA at room temperature for plane II (*ac**of site I at θ = 30˚ and *ab* of site II at θ = 50˚) , ν = 9.4060 GHz.

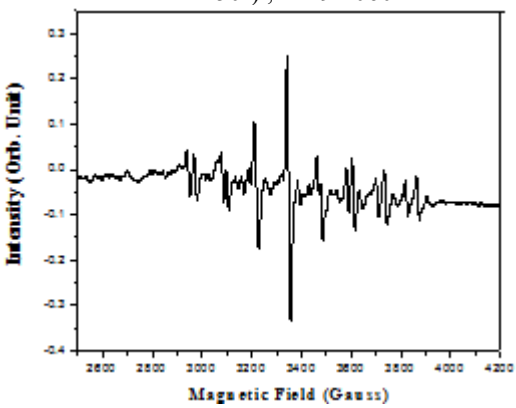

Figure 1(c): Single crystal EPR spectrum of VO(II)/TGA at room temperature for plane III (*ab* of site-I at θ = 110˚ and *bc** of site-II at θ = 10˚) , ν = 9.4060 GHz.

The EPR spectrum of the powder sample of VO(II)/TGA, recorded at room temperature, is given in Fig. 3. The spin Hamiltonian parameters calculated from the powder spectrum are also given in Table 3. The agreement between these values and the values obtained from single crystal analysis is relatively good. However, g_{xx}/g_{yy} and A_{xx}/A_{yy} are not resolved in powder spectrum due to the closeness in their values. This kind of observation is very common in VO(II) impurities. The principal values of the spin-Hamiltonian parameters of VO(II) ion in TGA are tabulated with similar lattices in Table 3.

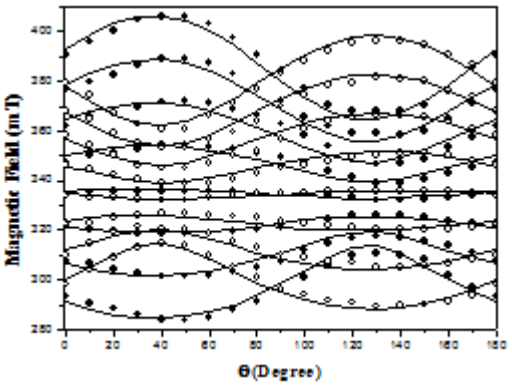

Figure 2 (a): The angular variation plot of VO(II)/ TGA at room temperature for plane *ac**. (⁻●-●- Indicates site I and –o-o- indicates site II). ν = 9.4060 GHz.

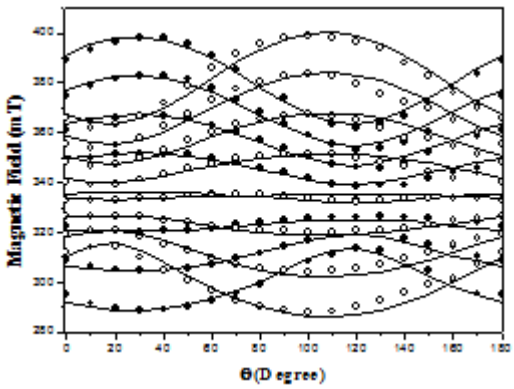

Figure 2 (b): The angular variation plot of VO(II)/ TGA at room temperature for plane *ac**. (⁻●-●- Indicates site I and –o-o- indicates site II). ν = 9.4060 GHz.

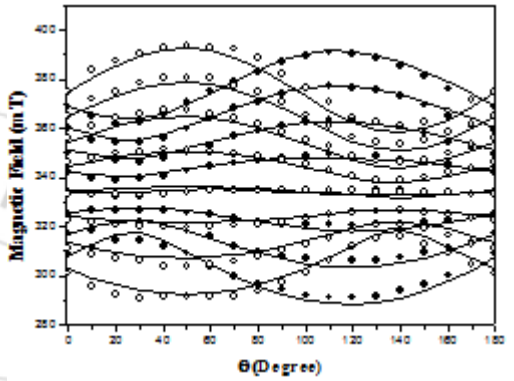

Figure 2 (c): The angular variation plot of Cu(II)/ TGA at room temperature for plane *ab*. (⁻●-●- Indicates site I and –o-o- indicates site II). ν = 9.4060 GHz.

Table 1 Principal values and direction cosines of *g* and *A* matrices for VO(II)/TGA at room temperature.

g/A			*Principal values*	*Direction cosines*		
				a	*b*	*c**
Site I						
g matrix						
1.9596	0.0000	-0.0177	1.9818	0.4833	0.6321	-0.6055
	1.9684	-0.0140	1.9646	0.6823	-0.7054	-0.1918
		1.9530	1.9346	-0.5484	-0.3204	-0.7722
A matrix (mT)						
7.590	0.000	9.701	-7.295	0.4797	0.4775	-0.7360
	5.538	8.325	6.396	0.6400	-0.7643	-0.0787
		4.428	18.456	0.6002	0.4333	0.6722
Site II						
g matrix						
1.9660	-0.0160	0.0146	1.9815	0.8005	-0.5439	0.2514
	1.9629	0.0109	1.9713	-0.1882	-0.6265	-0.7562
		1.9586	1.9348	0.5689	0.5581	-0.6039
A matrix (mT)						
8.819	3.620	-3.516	5.609	0.7332	-0. 6792	0.0299
	9.697	-4.085	7.140	-0.4802	-0.4863	-0.7299
		12.175	17.942	-0.4812	-0. 5496	-0.6828

Table 2: Direction cosines of bonds in TGA

Bond	*Direction cosines*		
	a	*b*	*c**
C(1) – O(1)	0.6658	-0.2917	0.6868
C(1) – O(2)	-0.9731	0.1598	0.1659
C(1) – C(2)	0.3358	0.1588	-0.9284
C(2) – N(1)	0.8798	-0.4482	-0.1582

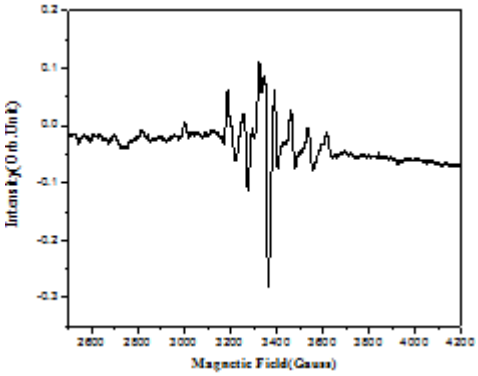

Figure 3: Powder EPR spectrum of VO(II) doped TGA recorded at RT. ν = 9.4022 GHz. Powder values are given in Table 3.

Table 3: Spin-Hamiltonian parameters for VO(II)/TGA

Host Lattices	g_{xx}	g_{yy}	g_{zz}	A_{zz} (mT)	A_{yy} (mT)	A_{xx} (mT)
TGA						
Site(I)	1.9818	1.9646	1.9346	18.456	6.396	7.295
Site(II)	1.9815	1.9713	1.9348	17.942	7.140	5.609
Powder	1.9758	1.9387	1.9387	18.600	6.050	6.050

3.1 Admixture coefficients

The admixture coefficients are calculated from the spin-Hamiltonian parameters. The single unpaired electron on the metal ion occupies d_{xy} or d_{xz} or d_{yz} orbital in an octahedral configuration. Upon lowering the symmetry, the ground state d_{xy} can mix with $d_{x^2-y^2}$, d_{yz} and d_{xz}. The admixture coefficients C_1, C_2 and C_3 are related to the spin-Hamiltonian parameters by the relations [19]

$$g_{\parallel} = 2\left(3C_1^2 - C_2^2 - 2C_3^2\right)$$

$$g_{\perp} = 4C_1\left(C_2 - C_3\right)$$

The equations (3.2) and (3.3) along with the normalization condition $\left(C_1^2 + C_2^2 + C_3^2 = 1\right)$ can be solved iteratively to obtain the admixture coefficients. The values of C_1, C_2, and C_3 obtained are given in Table 4, along with few literature values.

3.2 Optical absorption studies

The optical absorption spectrum of VO(II) doped in TGA at room temperature is shown in Fig. 4. The spectrum consists of three absorption bands at 230 nm (43,478 cm^{-1}), 521 nm (19,193 cm^{-1}) and 930 nm (10,752 cm^{-1}) respectively. VO(II) ion with d^1 configuration has ^2D ground state. In octahedral crystal field, the ^2D state splits into $^2T_{2g}$ and ^2E_g, while an octahedral field with tetragonal distortion further splits the $^2T_{2g}$ level into $^2B_{2g}$ and ^2E_g and ^2E_g splits into $^2B_{1g}$ and $^2A_{1g}$. The ordering of the levels will be $^2B_{2g} < {}^2E_g < {}^2B_{1g} < {}^2A_{1g}$ [19]. For vanadyl ion one can expect three bands corresponding to the transitions $^2B_{2g} \rightarrow {}^2E_g$ ($Ed_{xy} \rightarrow d_{xz}, d_{yz}$), $^2B_{2g} \rightarrow {}^2B_{1g}$ ($Ed_{xy} \rightarrow d_{x^2-y^2}$) and $^2B_{2g}$-$^2A_{1g}$ ($d_{xy} \rightarrow d_{z^2}$) [20, 21]. Among these levels, B_{2g} will be the ground state. Thus, for VO(II), two

Table 4: Admixture coefficients of VO(II) ion in TGA

Systems	C_1	C_2	C_3	κ	$P \times 10^{-4}$ (cm^{-1})	Ref.
TGA	0.7019	0.7111	0.0404	0.71	137.0	Present work
$Li_2SO_4 \cdot H_2O$	0.7060	0.7077	0.0378	0.88	121.0	[28]
$Zn(AP)(NO_3)_2$	0.7007	0.7135	0.0085	0.83	116.0	[29]
Apophyllite	0.7018	0.7124	0.0529	0.86	122.7	[30]
MPSH	0.7000	0.7130	0.0404	0.85	133.1	[31]

bands are expected corresponding to the transitions $^2B_{2g} \rightarrow {}^2E_g$ and $^2B_{2g} \rightarrow {}^2B_{1g}$. These two bands can be assigned to $\Delta_{\perp} = {}^2B_{2g} \rightarrow {}^2E_g$ ($Ed_{xy} \rightarrow d_{xz}, d_{yz}$) and $\Delta_{\parallel} = {}^2B_{2g} \rightarrow {}^2B_{1g}$ ($Ed_{xy} \rightarrow d_{x^2-y^2}$) transitions respectively. Except for the high – energy band at 43,478 cm^{-1}, all other bands are attributed as d-d transitions. The band at 43,478 cm^{-1} is due to charge transfer, arising from the promotion of electron from the filled bonding level (oxygen orbital) e_{π}^{b} to nonbonding level b_2 and is assigned to the transition $e_{\pi}^{b} \rightarrow {}^2B_{2g}(b_2)$ (from filled level to d_{xy} level) [22].

Both EPR and optical data can be used to calculate the molecular orbital coefficients by using following equations [23, 24]

$$g_{\parallel} = g_e\left[1 - \frac{4\lambda\beta_1^2\beta_2^2}{\Delta_{\parallel}}\right],$$

$$g_{\perp} = g_e\left[1 - \frac{\lambda\gamma^2\beta_2^2}{\Delta_{\perp}}\right],$$

Here g_e is free electron g value equal to 2.0023 and λ is the free ion value of the spin-orbit coupling constant of VO(II) ion (170 cm^{-1} [25]). β_1^2, β_2^2 and γ^2 are the molecular orbital coefficients of the d^1 electron. These molecular orbital coefficients (also called bonding coefficients) thus characterize in-plane σ bonding, in-plane π bonding and out-of-plane π bonding, respectively.

The parallel and perpendicular components of hyperfine interaction $A_{\parallel}$ and $A_{\perp}$ are related to the molecular orbital coefficients by the following expressions [26],

$A_{\parallel} = -P[\kappa - 4/7\,\beta_2^2 - (g_e - g_{\parallel}) - 3/7(g_e - g_{\perp})]$ (a)

$A_{\perp} = -P[\kappa - 2/7\,\beta_2^2 - 11/14\,(g_e - g_{\perp})]$ (b)

The degrees of distortion can be estimated from the Fermi contact term κ and the P parameter, which are related to radial distribution of wave function of the ions given as $P = g_e g_N \beta_e \beta_N \langle r^{-3} \rangle$. Here, β_2^2 is the covalence ratio of V=O bonds. The parameter P is related to the isotropic hyperfine

coupling and represents the amount of unpaired electron density at the nucleus.

Neglecting the second order effects and taking negative values for $A_{\parallel}$ and $A_{\perp}$, P value is calculated from the following equation [27] and the results are given in Table 4.

$P = 7(A_{\parallel} - A_{\perp}) / 6 + (3/2)(\lambda/\Delta_{\parallel})$

The Fermi contact parameter (κ) is calculated by using the equation

$\kappa = - A_{iso} / P - (g_e - g_{iso})$

Here, A_{iso} and g_{iso} are calculated from the powder A and g values respectively. Combine equations (a) and (b) and eliminating κ, one can get an expression for β_2^2 in terms of the principal values of the g and A tensors,

$\beta_2^2 = (-7/6)[(A_{\parallel} - A_{\perp})/P + (g_e - g_{\parallel}) - (5/14)(g_e - g_{\perp})]$

The calculated molecular orbital coefficient parameters are given in Table 5. The deviation of β_1^2 from unity usually represents the degree of the admixture of the ligand orbitals and increase in the degree of covalency. β_2^2, found in this work, clearly indicates that the bonding is nearly ionic and represents poor π bonding of the ligands. If $\beta_1^2 = 1$, the bond would be completely ionic. If $\beta_1^2 = 0.5$, the bond would be completely covalent. The parameters $1 - \beta_1^2$ and $1 - \gamma^2$ are the measures of the covalency. First term gives an indication of the influence of σ bonding between vanadium atom and equatorial ligands, second indicates the influence of π bonding between the vanadium ion and the vanadyl oxygen.

Table 5: Molecular orbital coefficients for VO(II) ion doped in TGA

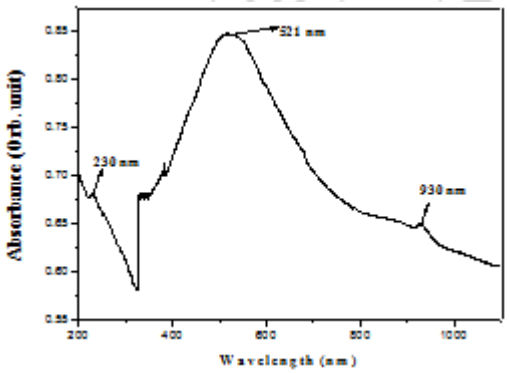

Figure 4: Optical absorption spectrum of VO(II) doped TGA recorded at room temperature

4. Conclusion

EPR and optical studies of vanadyl ions in TGA single crystal have been carried out at room temperature. The g and A parameters and their direction cosines have been evaluated from EPR analysis. The detailed EPR analysis indicates that the two vanadyl sites occupy interstitial positions in the crystal lattice. The crystal field and tetragonal distortion parameters have been estimated by assigning the optical transitions. From the correlation of EPR and optical data different bonding parameters have been determined.

References

[1] I. Ledoux, Synthetic Metal, 54 (1993) 123.
[2] D. R.Yuan, D. Xu, N. Zang, M.G. Liu, M.H. Jiang, Chain, Phys. Let., 13 (1996) 841.
[3] M. Iwai, T. Kobayashi, H. Furuya, Y. Mori, T. Sasaki, J. Appl. Phys., 36 (1997) 276.
[4] D. Bravo, F.J. Lopez, Opt. Mater. 13 (1999) 141.
[5] P. Gunter, J. P. Huignard, Photorefractive Materials and Their Applications, Vol.1, Springer, Berlin, 1987.
[6] M.H. Jiang, Q. Fang, Adv. Mater. 11 (1999) 1147.
[7] D. Bravo, F.J. Lopez, Optical Materials 1999, 13, 141-145.
[8] P. Gunter, J.P. Huignard, Photorefractive Materials and Their Applications, vol. I, Springer, Berlin, 1987.
[9] Th. Nolte, Th. Pawlik, J.M. Spaeth, Solid State Communications 1997, 104, 535-539.
[10] I. Selbin, The chemistry of oxovanadium(IV). Chem. Rev. 1965, 65, 153–175.
[11] L. S. Prasad, S. Subramanian, J. Chem. Phys. 1987, 86, 629–633.
[12] C. K. Jorgenson, Acta Chem. Scand. 1995, 11, 73–85.
[13] C. J. Ballhausen, H. B. Gray, Inorg. Chem. 1962, 1, 111–122.
[14] T. R. Ortolano, J. Selbin, S. P. McGlynn, J. Chem. Phys. 1964, 41, 262–268.
[15] L. G. Vanquickenborne, S. P. Mc.Glynn, Theor. Chim. Acta 1968, 9, 390–400.
[16] W. L. Feng, Phil. Mag. 2009, 89, 1391–1394.
[17] S.S. Hussaini, N.R. Dhumane, V.G. Dongre, M.D. Shirsat , Materials Science-Poland 2009, 27, 365-372.
[18] F. Clark, R.S. Dickson, O. B. Fulton, J. Isoya, A. Lent, D. G. Mc Gavin, M. J. Mombourquette, R. H. D. Nuttall, P. S. Rao, H. Rinnerberg, W.C. Tennant, J. A. Weil, EPR-NMR Program, University of Saskatchewan, Saskatoon, Canada, 1996.
[19] K. Ramesh, V. Somasebharan, S.N. Rao, R.Y.P. Reddy, Phys. Scr. 35 (1987) 40.
[20] C.J. Ballhausen, H.B. Gray, Inorg. Chem. 1 (1962) 111.
[21] T.R. Ortolano, J. Selbin, S.P. McGlynn, J. Chem. Phys. 41 (1964) 262.
[22] V.P. Seth, S.K. Yadav, V.K. Jain, Pramana, J. Phys., 21 (1983) 65.
[23] A.B.P. Lever, "Inorganic Electronic Spectroscopy", 2nd Ed., Elsevier, New York, 1986.
[24] V.P. Seth, S. Gupta, A. Jindal, S.K. Gupta, J. Non-Cryst. Solids, 162 (1993) 263.
[25] R. Muncaster, S. Parke, J. Non-Cryst., 24 (1977) 399.
[26] C.J. Ballhausen, H.B. Gray B, Inorg. Chem., 1 (1961) 111.
[27] D. Pathinettam Padiyan, C. Muthukrishnan, R. Murugesan, J. Mol. Struct., 648 (2003) 1.
[28] U.B. Gangadharmath, S.M. Annigeri, A.D. Naik, V.K. Revankar, V.B. Mahale, J. Mol. Struct., 572 (2000) 61.
[29] C. Muralikrishna, Ph.D. Thesis, Indian Institute of Technology, Madras, India, 1984.
[30] L.S. Prasad, Ph.D. Thesis, Indian Institute of Technology, Madras, India, 1986.
[31] G. Ramakrishnan, M.B.V.L.N. Swamy, P. Sambasiva Rao, S. Subramanian, Proc. Indian Acad. Sci. (Chem. Sci.) 103 (1991) 613.

[32] H. Anandalakshmi, T.M. Rajendiran, R. Venkatesan, P. Sambasiva Rao, Spect. Chim. Acta A 56 (2000) 2617-2625.
[33] B.D.P. Raju, K.V.Narasimhulu, N.O. Gopal, J.L. Rao, J. Phys. Chem. Solids 64 (2003) 1339.